

ORIGINAL ARTICLE

Whole-genome sequencing of chronic lymphocytic leukaemia reveals distinct differences in the mutational landscape between IgHV^{mut} and IgHV^{unmut} subgroups

This article has been corrected since Advance Online Publication and a corrigendum is also printed in this issue

A Burns^{1,2,12}, R Alsolami^{1,3,4,12}, J Becq⁵, B Stamatopoulos^{1,12}, A Timbs¹, D Bruce^{2,6}, P Robbe^{1,2}, D Vavoulis^{1,2}, R Clifford^{2,12}, M Cables¹, H Dreau¹, J Taylor⁷, SJL Knight⁷, R Mansson⁸, D Bentley⁵, R Beekman⁹, JI Martín-Subero⁹, E Campo¹⁰, RS Houlston¹¹, KE Ridout^{1,2,13} and A Schuh^{1,2,6,13}

Chronic lymphocytic leukaemia (CLL) consists of two biologically and clinically distinct subtypes defined by the abundance of somatic hypermutation (SHM) affecting the Ig variable heavy-chain locus (IgHV). The molecular mechanisms underlying these subtypes are incompletely understood. Here, we present a comprehensive whole-genome sequencing analysis of somatically acquired genetic events from 46 CLL patients, including a systematic comparison of coding and non-coding single-nucleotide variants, copy number variants and structural variants, regions of kataegis and mutation signatures between IgHV^{mut} and IgHV^{unmut} subtypes. We demonstrate that one-quarter of non-coding mutations in regions of kataegis outside the Ig loci are located in genes relevant to CLL. We show that non-coding mutations in *ATM* may negatively impact on *ATM* expression and find non-coding and regulatory region mutations in *TCL1A*, and in IgHV^{unmut} CLL in *IKZF3*, *SAMHD1*, *PAX5* and *BIRC3*. Finally, we show that IgHV^{unmut} CLL is dominated by coding mutations in driver genes and an aging signature, whereas IgHV^{mut} CLL has a high incidence of promoter and enhancer mutations caused by aberrant activation-induced cytidine deaminase activity. Taken together, our data support the hypothesis that differences in clinical outcome and biological characteristics between the two subgroups might reflect differences in mutation distribution, incidence and distinct underlying mutagenic mechanisms.

Leukemia (2018) 32, 332–342; doi:10.1038/leu.2017.177

INTRODUCTION

Chronic lymphocytic leukaemia (CLL) is the most common form of adult leukaemia in the Western world,¹ accounting for one-third of new cases of leukaemia each year.² CLL is characterised by significant clinical heterogeneity. While one-third of patients never require any treatment, others invariably progress and ultimately develop chemorefractoriness. This clinical heterogeneity is reflected at least in part by characteristic biological features. Chromosomal deletions and amplifications are among the most common genomic aberrations described in CLL³ and have been associated with diverse phenotypes and contrasting clinical behaviour.⁴

Genome^{5,6} and exome-wide⁷ sequencing efforts have identified a number of recurrent acquired mutations in the coding regions of genes. Mutations in the coding regions of *TP53*,^{8–10} *SF3B1*,^{7,11,12} *NOTCH1*,^{13–15} *RPS15*¹⁶ and *SAMHD1*¹⁷ have been associated with chemorefractoriness, advanced disease, poor prognosis and/or transformation to high-grade lymphoma.

A recent study, using a combination of whole-genome sequencing (WGS) and whole-exome sequencing, addressed for the first time the

potential significance of non-coding mutations in CLL¹⁸ and, in doing so, characterised a region of kataegis affecting an enhancer site 300 kb upstream of the *PAX5* gene. Kataegis is characterised by hotspots of somatically acquired mutations that are scattered throughout the genome. The study also described splice-site mutations in *NOTCH1*, which have since been correlated with clinical outcome.¹⁹ The study illustrates the potential of WGS to reveal important driver mutations outside the protein-coding regions.

During B-cell development, somatic point mutations are introduced at the Ig variable gene loci via the action of activation-induced cytidine deaminase (AID). CLL is divided into two distinct subgroups: those with little or no somatic hypermutation (SHM) and unmutated Ig variable heavy-chain locus (IgHV^{unmut}), defined by $\geq 98\%$ homology to the germline IgHV sequence, and those with IgHV hypermutated CLL (IgHV^{mut}) ($< 98\%$ germline homology). IgHV^{mut} patients have significantly better treatment-free and overall survival than IgHV^{unmut} patients.²⁰ Importantly, there is accumulating evidence that at least a proportion of IgHV^{mut} patients might achieve cure

¹Department of Molecular Haematology, Oxford Molecular Diagnostics Centre, John Radcliffe Hospital, Oxford, UK; ²Department of Oncology, University of Oxford, Oxford, UK; ³Nuffield Department of Clinical Laboratory Sciences, University of Oxford, Oxford, UK; ⁴King Abdulaziz University, Faculty of Applied Medical Sciences, Jeddah, Saudi Arabia; ⁵Illumina Cambridge Ltd, Saffron Walden, UK; ⁶Department of Haematology, Oxford University Hospitals NHS Trust, Oxford, UK; ⁷Wellcome Trust Centre for Human Genetics, University of Oxford, Oxford, UK; ⁸Center for Hematology and Regenerative Medicine Huddinge, Karolinska Institute, Stockholm, Sweden; ⁹Biomedical Epigenomics Group, Institut d'Investigacions Biomèdiques August Pi i Sunyer (IDIBAPS), University of Barcelona, Barcelona, Spain; ¹⁰Hematopathology Unit, Hospital Clinic, Institut d'Investigacions Biomèdiques August Pi i Sunyer (IDIBAPS), University of Barcelona, Barcelona, Spain and ¹¹Division of Molecular Pathology, the Institute of Cancer Research, London, UK. Correspondence: Professor A Schuh, Department of Molecular Haematology, Oxford Molecular Diagnostics Centre, Level 4, John Radcliffe Hospital, Oxford, OX3 9DU, UK. E-mail: anna.schuh@oncology.ox.ac.uk

¹²These authors contributed equally to this work.

¹³These senior authors contributed equally to this work.

Received 9 January 2017; revised 18 April 2017; accepted 17 May 2017; accepted article preview online 6 June 2017; advance online publication, 27 June 2017

following chemoimmunotherapy.^{21,22} Using targeted deep sequencing of the IgHV locus, our group recently demonstrated that 25% of CLL carry additional small IgHV subclones that further refine the prognostic value of the IgHV status.²³ IgHV^{unmut} and IgHV^{mut} CLL also differ in their gene expression^{24,25} and genome-wide methylation profiles.²⁶ These differences in transcriptional output and clinical behaviour might be due to differences in B-cell receptor signalling response to antigens.²⁷ Alternatively, cell-autonomous and antigen-independent signalling could be a crucial pathogenic mechanism in both types of CLL, independent of IgHV status.²⁸

Recent WGS studies have identified various mutation signatures in CLL,^{29,30} including AID- and aging-related signatures, and there is evidence for the full range of AID activity in both IgHV^{unmut} and IgHV^{mut} CLL.³¹ We therefore hypothesised that the clinical and biological differences seen might be due to differences in the activity and target loci of AID and/or other mutagenic mechanisms between these two groups. One previous study examined mutation signatures in good-risk CLL with isolated deletion of 13q and IgHV^{mut}.³² Here, we therefore included patients with IgHV^{unmut} poor-risk CLL and compared the coding and non-coding mutation spectrum between the two groups. To perform a more rigorous analysis of the non-coding space, we used experimentally determined CLL-specific chromatin immunoprecipitation followed by high-throughput sequencing (ChIP-seq) and assay for transposase-accessible chromatin with high-throughput sequencing (ATAC-seq) data in combination with existing data from the ENCODE project^{33,34} to produce bespoke non-coding annotations. We then developed an *in silico* annotation pipeline for these mutations that included the identification of regions of kataegis, and revealed distinct patterns in the occurrence and distribution of mutations between IgHV^{unmut} and IgHV^{mut} subgroups. From our experimental data, we also identify non-coding and mutations in regulatory elements of known cancer-related genes that we link to IgHV^{unmut} CLL. Finally, we show the potential association of these non-coding mutations with gene expression using paired RNA-seq data from the same patients. Taken together, our data support the hypothesis that the difference in clinical outcomes observed between IgHV^{unmut} and IgHV^{mut} is due, at least in part, to differences in the genomic footprint between these two subgroups. Further, it reveals known cancer-linked genes frequently mutated in the IgHV^{unmut} subtype that may be candidates for a deeper understanding of these differences.

PATIENTS AND METHODS

Patient and sample characteristics

We isolated tumour and germline DNA from peripheral blood and saliva samples, respectively, of 46 CLL patients diagnosed at the Oxford University Hospitals, Oxford, or the Karolinska Institute, Stockholm. Informed consent was obtained in line with the Declaration of Helsinki and local research ethics committees. The median age was 69 (range 49–94) years. Fifty-nine per cent (27/46) were male. Sixteen cases were IgHV^{mut} and 27 were IgHV^{unmut}. Patients with the IgHV 3–21 rearrangement have been shown to display the same poor prognostic indications as those with unmutated Ig genes.³⁵ Thus, three cases with < 98% homology to the Ig germline sequence, harbouring the V3–21 rearrangement, were also classified as IgHV^{unmut}. Of the 16 IgHV^{mut} patients, 5 were refractory and 11 naïve, and of the 30 IgHV^{unmut} samples, 17 were refractory and 13 naïve. We also subjected 31 samples to targeted deep sequencing of the IgHV gene as described previously.²³ Eight patients had been treated with at least one round of chemotherapy before WGS (Supplementary Figures 5 and 6). Twenty-two cases developed chemorefractoriness subsequent to sequencing, defined by either relapse \leq 24 months following initial treatment or the presence of *TP53* disruption. Twenty-two were chemosensitive, while the status of the remaining two was unknown (Supplementary Table 1).

WGS and annotation

Matched tumour and germline WGS libraries were prepared from 2 μ g DNA using the TruSeq DNA PCR Free Library Preparation Kit (Illumina, San Diego, CA, USA). Libraries were subjected to 2 \times 35 bp paired-end sequencing on a HiSeq 2500 instrument (Illumina), to a mean sequencing depth of 39x for tumour (range 35–54) and 36x for germline (range 28–54) samples. Alignment of sequencing reads to the hg19 human genome build was performed using iSAAC v.01.13.04.04.³⁶ SNVs and indels were called using Starling v.2.0.3 and Strelka v.2.0.10.³⁷ Germline mutations were subtracted from the matched tumour and filtered and annotated using our in-house pipeline (Supplementary Methods).

Experimentally determined CLL-specific epigenetics data was generated in the context of the Blueprint Project by ATAC-seq and ChIP-seq on six histone modification marks with non-overlapping functions (H3K4me3, H3K27ac, H3K4me1, H3K27me3, H3K36me3 and H3K9me3). Both methods were performed according to standard protocols available through the Blueprint Portal (<http://www.blueprint-epigenome.eu/index.cfm?p=7BF8A4B6-F4FE-861A-2AD57A08D63D0B58>). Chromatin states were identified using the chromHMM Software,³⁸ and include Active Promoter, Weak Promoter, Poised Promoter, Strong Enhancer, Weak Enhancer, Transcription Transition, Transcription Elongation, Weak Transcription and Heterochromatin (Supplementary Methods).

Whole transcriptome sequencing

Whole transcriptome sequencing libraries were prepared using the TruSeq Stranded Total RNA Sample Preparation Kit (Illumina). Libraries underwent 2 \times 76 bp paired-end sequencing on a HiSeq 2500 instrument (Illumina). Sequence data was aligned to the hg19 build of the human genome using TopHat.³⁹

Data analysis

Copy number alterations (CNAs) and structural rearrangements were identified using Nexus (Biodiscovery Inc., El Segundo, CA, USA) and DELLY,⁴⁰ respectively. Regions of kataegis within individual patients were identified using methods described previously.⁴¹ A further in-house pipeline was used to identify regions of higher mutational load across the cohort (Supplementary Methods). The presence of mutational signatures were determined using methods described previously.^{42,43} (Supplementary Methods).

Statistical analysis

Statistical analyses were performed using SPSS version 22 (IBM, Armonk, NY, USA) and Prism version 5 (GraphPad, La Jolla, CA, USA). Categorical variables were compared using either the χ^2 test or Fisher's exact test as appropriate. Survival analysis was performed using the Kaplan–Meier method. *P*-values were considered significant at the 0.05 level.

RESULTS

Somatic mutation distribution and density

After imposing a rigorous QC step, the number of *bona fide* mutations per tumour ranged from 516 to 2697 per sample (median, 1426) (Figure 1a and Supplementary Table 2), corresponding to a mean mutation rate of 0.49 ± 0.16 per megabase (range 0.17–0.9). Of these, 823 missense, 62 nonsense and 85 splice-site mutations occurred in protein-coding regions. Of the 3260 insertion/deletions detected across the genomes, 62 affected protein-coding regions. While the overall mutation rate outside the Ig loci was higher in IgHV^{mut} tumours compared with that in IgHV^{unmut} samples ($P=0.0089$, unpaired *t*-test; Figure 1b), there was no difference across all coding regions ($P=0.1191$, unpaired *t*-test). IgHV^{unmut} cases did, however, show an enrichment for coding mutations in the known CLL driver genes^{16,44} ($P=0.0380$, unpaired *t*-test; Figure 1c), consistent with a more aggressive phenotype. Furthermore, upon examining the genomic context of the mutations, we discovered significant enrichment for variants within gene promoter regions in IgHV^{mut} patients ($P<0.0001$, unpaired *t*-test; Figures 1d and e).

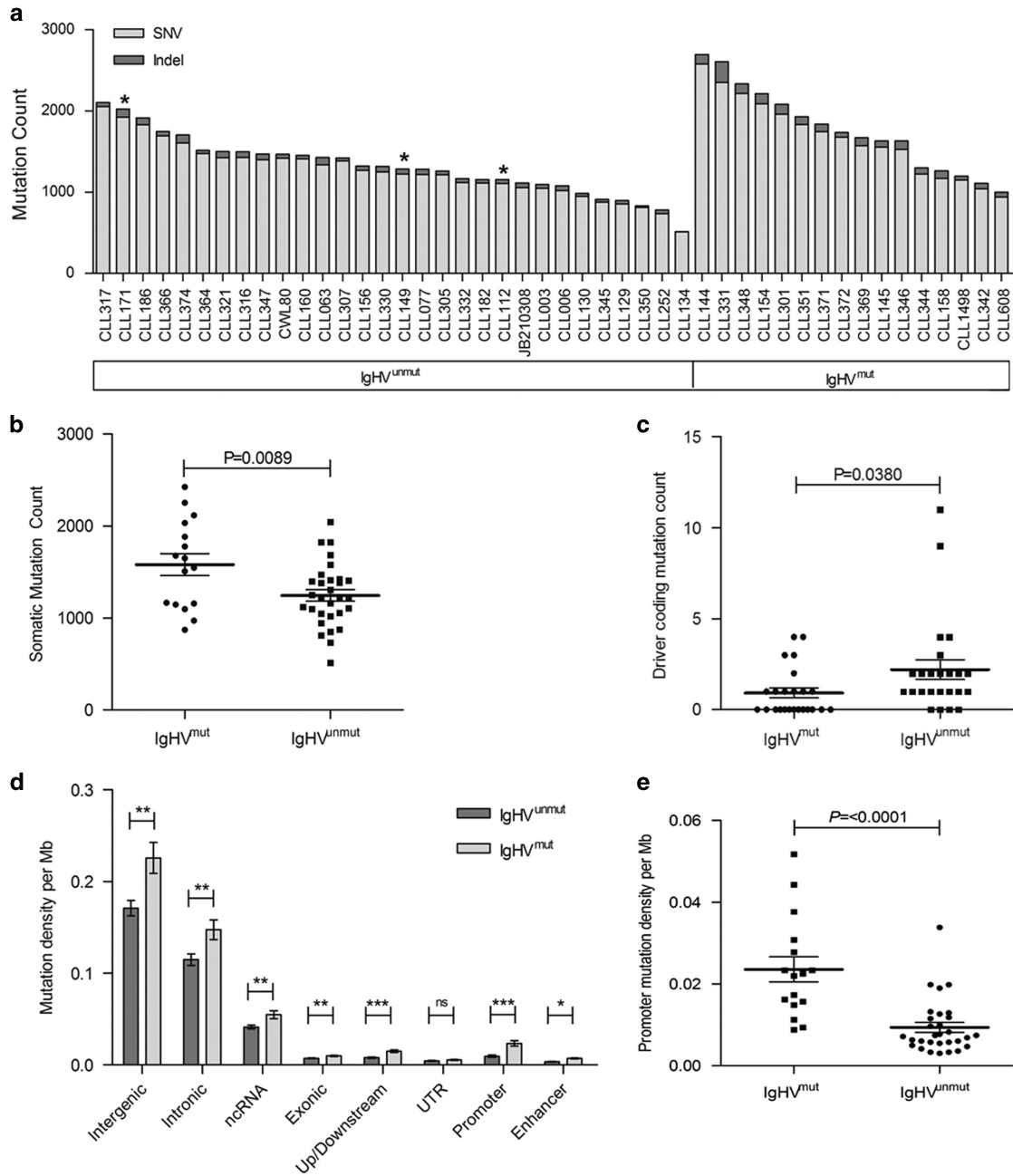


Figure 1. Overview of the mutational landscape in IgHV^{mut} and IgHV^{unmut} CLL. (a) Total number of SNVs and indels per sample and by IgHV mutation status. Asterisks denote cases with IgHV 3-21 rearrangement. (b) Dot plot of total somatic mutation count between IgHV subgroups. Patients with IgHV^{mut} CLL harbour higher total mutational load, but reduced driver coding (c) and higher promoter variant counts (d and e) than IgHV^{unmut} CLL. Error bars show \pm s.e.m.

Copy number alterations

Thirty-five of the 46 CLL cases (76%) harboured at least one CNA (median, 2) (Figure 2 and Supplementary Table 3), with IgHV^{unmut} tumours tending to feature more CNAs than IgHV^{mut} cases (1.3 vs 0.8 per sample, $P=0.0651$). The most frequent recurrent CNAs were del(13q) (41%, 19/46), del(11q) (20%, 9/46) and del(17p) (20%, 9/46). Trisomy 12 was seen in 20% of tumours (9/46). Seventy-eight per cent of del(17p) cases were IgHV^{unmut}. The minimally deleted region at del(11q) encompassed *ATM*, with four tumours also carrying *ATM* mutations (two IgHV^{mut}, two IgHV^{unmut}). Partial or full gain of 2p⁴⁵ (70–90.5 Mb) was seen in three tumours, but was not associated with differential expression of *REL*, *ALK* or *MYCN*,

which mapped to the minimally deleted region. Del(8p) was also seen in three patients (CLL364, CLL154 and CLL372). It was noteworthy that del(8q) was associated with other CNAs—del(11q), gain(12) and del(17p) (CLL364), del(11q) and del(17p) (CLL372) and del(13q) (CLL154). This concurs with other studies, which have reported that del8p deletions often coexist with other CNAs.^{46,47} Tumour CLL364 was also the only one to display chromothripsis.

Structural variants

We detected 79 interchromosomal translocations in the tumours from 30 of the 46 patients (average of 1.7 per case, range 1–9; Figure 2 and Supplementary Table 4). Seventeen of the 79 events

Table 1. Regions of kataegis affecting gene regulatory and exonic regions in individual CLL cases

Patient ID	IgHV status	Chr.	Start (bp)	End (bp)	No. of mutations	Affected genes
CLL156	Unmutated	2	140 885 911	141 045 820	8	LRP1B
CLL154	Mutated	3	157 290 339	157 295 704	6	PQLC2L
CLL348	Mutated	3	183 273 058	183 273 364	6	KLHL6
CLL063	Unmutated	5	21 810 369	21 843 504	9	CDH12
CLL301	Mutated	7	122 433 699	122 517 296	12	CADPS2
CLL301	Mutated	7	122 622 586	122 638 447	6	TAS2R16
CLL351	Mutated	9	123 416 699	123 479 606	43	MEGF9
CLL144	Mutated	11	108 121 624	108 129 499	9	ATM
CLL307	Unmutated	13	51 664 141	51 665 954	6	LINC00371
CLL156	Unmutated	14	21 835 327	21 835 546	6	SUPT16H
CLL252	Unmutated	18	9 284 149	9 374 417	6	ANKRD12
CLL301	Mutated	18	60 873 525	60 988 029	12	BCL2
CLL348	Mutated	18	60 906 440	60 988 117	10	BCL2
CLL301	Mutated	X	98 765 633	98 769 284	10	XRCC6P5

Abbreviations: CLL, chronic lymphocytic leukaemia; IgHV, Ig variable heavy-chain locus.

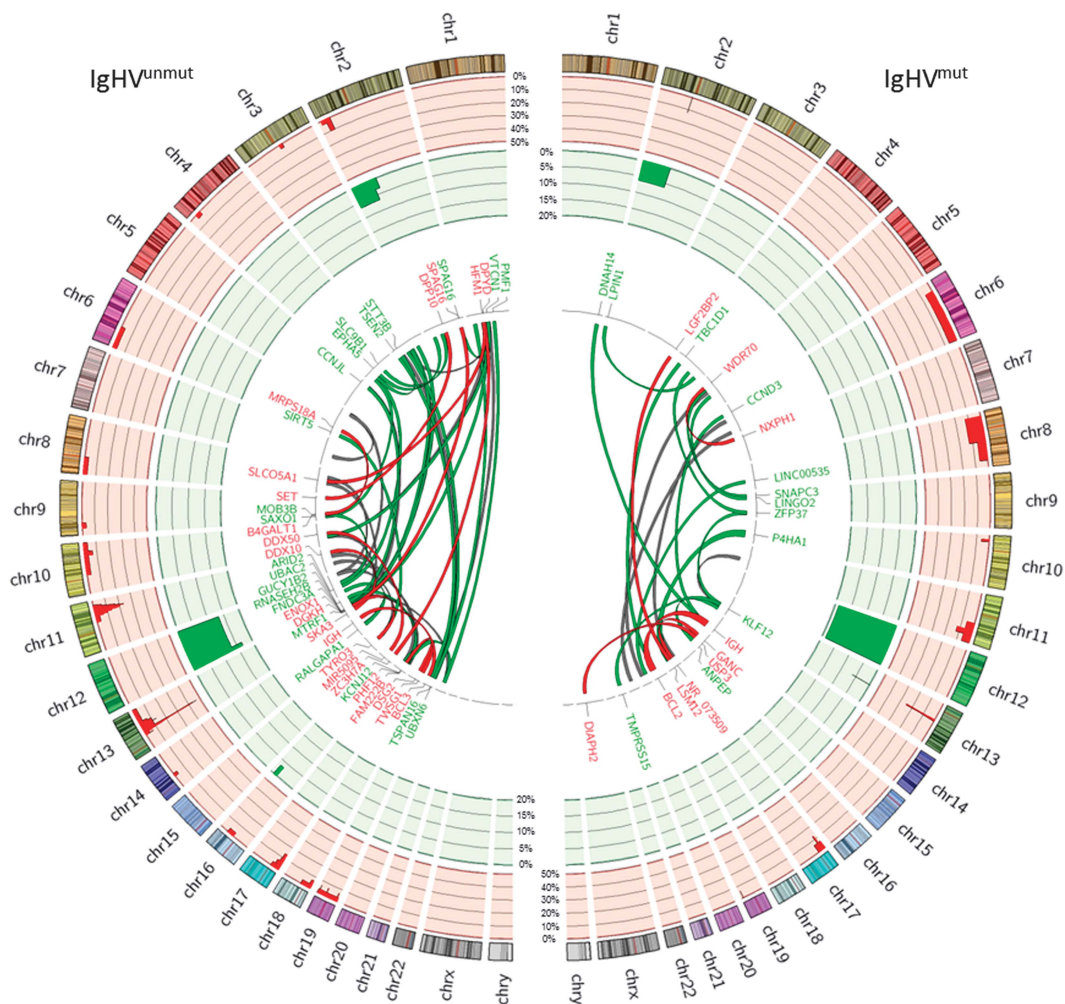


Figure 2. Structural rearrangements in IgHV^{unmut} and IgHV^{mut} CLL. Circos plot depicting the frequency and locations of CNAs and translocations detected in 46 CLL genomes. The two outermost tracks represent CNAs: CN loss (red) and CN gain (green). Copy number data is displayed as the percentage of each IgHV subgroup affected. The centre plot shows translocations identified in the cohort. Red links indicate tier 1 events (gene:gene), green links indicate tier 2 events (gene:intergenic) and grey indicate tier 3 (intergenic:intergenic). The widths of the bands are indicative of the number of patients affected by the translocation.

(22%) were predicted to generate gene fusion proteins (tier 1). Two IgHV^{mut} cases (CLL301 and CLL348) had *IGH/BCL2* t(14;18) fusions, and a single IgHV^{unmut} case had *IGH/BCL3* t(14;19). RNA-seq data was available in 22 out of the 30 patients (73%, 22/30).

The other interchromosomal translocations involved either the coding region of a gene (tier 2, 44%, 35/79) or intergenic regions (tier 3, 34%, 27/79). RNA expression supported the functional consequences of t(14;18) (*IGH/BCL2*), t(2;9) (*DPP10;SET*) and both

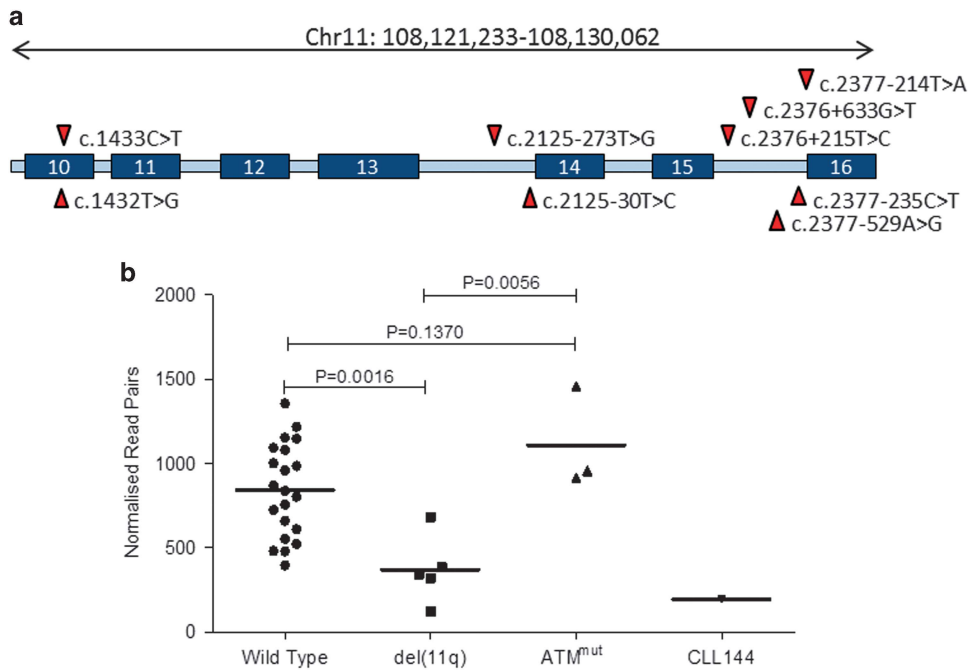


Figure 3. Kataegic *ATM* mutations in CLL144. (a) Graphical representation of *ATM* showing the distribution of kataegic mutations in CLL144. Blue boxes represent exonic regions of the *ATM* transcript. (b) Dot plot comparing the *ATM* transcript expression levels of CLL cases with no 11q disruption (wild type), those with del(11q), mutations in *ATM* (*ATM*^{mut}) and CLL144. Expression levels are shown as reads per million aligned reads. Error bars show \pm s.e.m.

t(1;2) and t(3;19), linking *SPAG16* and *UBXN6* to intergenic regions (Supplementary Figure 1).

Somatic mutation profiles

Coding mutations. As expected, somatic mutations in the coding regions of *SF3B1*, *TP53*, *ATM* and *NOTCH1* were the most frequent, occurring in 30.4% (14/46), 19.6% (9/46), 15.2% (7/46) and 13% (6/46) of patients, respectively. The missense Lys700Glu substitution in *SF3B1* (28%, 4/14), between the third and fifth HEAT domains, affected mainly IgHV^{unmut} patients, although this did not reach significance ($P=0.316$). Missense mutations were also the most frequent type found in *TP53* (82%, 9/11), occurring in the DNA-binding domain and in all previously described in the COSMIC database. Two cases harboured indels within *TP53*, one 4 bp deletion in exon 4 and one 19 bp deletion in exon 5. Again, *TP53* mutations were more common in IgHV^{unmut} patients (9/11, 82%), but not to a significant level ($P=0.463$). Seven cases contained eight mutations within the coding region of *ATM*, comprising six missense mutations, a 5 bp deletion in exon 53 and one stop gain mutation in exon 25, resulting in the loss of 60% of the coding sequence. Mutations in *NOTCH1* were confined to exon 34, with 71% (5/7) comprising the c.7541_7542delCT variant resulting in early termination of the PEST domain. In addition, we identified a number of low-frequency recurrent mutations. The tumour suppressor gene *FAT1* harboured protein-coding mutations in 11% of samples (5/46), encompassing both chemorefractory and untreated cases.⁴⁸ Most mutations in *FAT1* occurred within exon 2 (60%, 3/5), including a nonsense mutation at residue Lys125, resulting in the loss of >97% of the coding region. We detected five missense and two synonymous mutations in *KLHL6* across two patients. In one case, three mutations (Arg66Gly, Met67Thr and Val88Glu) were clustered close together in exon 1, and both cases were IgHV^{mut} as described previously.⁵ Other previously described candidate driver genes harboured low-frequency variants, including two mutations each in *MYD88*, *SAMHD1*, *DDX3X* and *BIRC3*, with one each in *FBXW7*, *XPO1*, *CHD2* and *POT1*.^{5,6,12,14,17,44}

Mutations in non-coding and regulatory regions. Localised regions of increased mutation density, also referred to as kataegis, have been described previously in other types of cancer. Here, we used both previously described methods⁴¹ and our own approaches to identify these regions in our cohort (Supplementary Methods).

To this end, we first examined each CLL genome individually, where we detected 74 kataegic regions across 31 samples affecting 14 chromosomes. Some chromosomal regions were recurrently affected, most notably, and as expected, those encoding the Ig light and heavy chains on chromosomes 2 (11/74, 15%), 14 (33/74, 45%) and 22 (13/74, 18%). These regions accounted for 88% (1397/1591) of all kataegic mutations. IgHV^{mut} cases harboured significantly more kataegic regions than IgHV^{unmut} cases ($P=0.0004$), a relationship that continued even after removing regions found at the Ig loci ($P=0.0308$). The 19 non-Ig regions occurred in 11 patients and ranged in length from 219 bp to 159 kbp. Fourteen were located within or across gene boundaries. Importantly, almost half of these (6/14, 43%) affected non-coding regions of genes were known to also carry coding mutations in CLL including *KLHL6*,⁵ *MEGF9*,⁴⁹ *CDH12*,⁴⁴ *CADPS2*,^{5,44} *LRP1B*^{44,49} and *ATM*^{50,51} (Table 1 and Supplementary Table 5).

In one IgHV^{mut} case, CLL144, a kataegic region was identified within *ATM*, comprising 10 mutations in a 9 kb span between exon 10 and intron 16. Eighty per cent (8/10) of the mutations occurred in intronic regions, with two more in exon 10. The two coding mutations affected adjacent bases, but resulted in a single serine to valine residue substitution (Ser478Val), predicted as tolerated by the sorting tolerant from intolerant algorithm. Experimentally determined ChIP-seq data revealed that all 10 mutations occurred in regions of strong H3K36 trimethylation, which is an indication of transcription elongation.³⁸ Analysis of paired RNA-seq data from CLL144 revealed a similarly reduced level of *ATM* expression as seen in cases harbouring del(11q). Furthermore, cases with del(11q) showed significantly lower *ATM* expression levels than *ATM* wild-type cases ($P=0.0016$), as expected⁵⁰ (Figure 3).

Sites of kataegis have been shown to colocalise with structural rearrangements.^{42,52} As such, the 19 kataegic regions that were

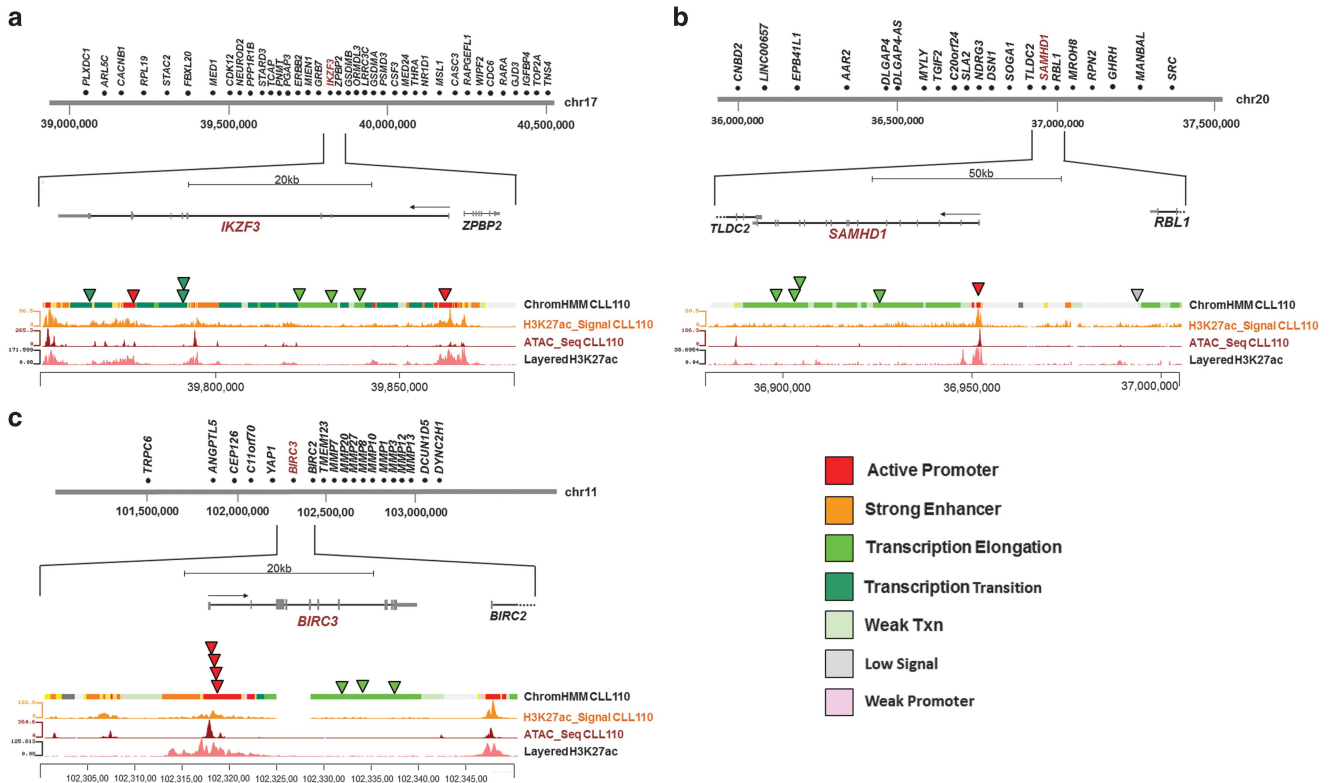


Figure 4. Non-coding mutations confirmed experimentally with ChIP-seq and ATAC-seq. Diagrams of non-coding mutations in three genes and the corresponding annotation data. All lower panels; correlation of mutation loci with H3K27Ac and ATAC-seq signal of CLL110 and ChromHMM annotation (all three layers obtained from experiments with primary CLL cells) and layered H3K27Ac data from the ENCODE database (GM12878). (a) *IKZF3* locus and surrounding region on chromosome 17, with the position of all mutations detected in our cohort, (b) *SAMHD1* locus and surrounding region on chromosome 20, with the position of all mutations detected in our cohort and (c) *BIRC3* locus and surrounding region on chromosome 11, with the position of all mutations detected in our cohort.

not at sites of SHM were correlated with CNAs and translocations. Five were found to be in close proximity to structural alteration events (Supplementary Table 6). In line with previous observations,^{42,52} this suggests that kataegis can indicate the presence of structural rearrangements.

Second, we combined the WGS data from all 46 CLL samples, and used a combination of methods to highlight strict regions of kataegis, alongside wider mutational hotspots (Supplementary Methods). Through this approach, we identified 159 additional kataegic regions, which were further annotated for the presence of coding and non-coding regulatory regions using a combination of functional data obtained from normal B cells, CLL cell lines and primary CLL. Sites were defined as active regulatory regions if they fell within chromatin states containing H3K27 acetylation (that is, active promoters, strong enhancers or transcription transition), as determined using the CLL-specific ChIP-seq data (see Supplementary Methods). With the exception of the 9q34.3 locus of *NOTCH1*, 51 regions were excluded from further analysis because of their centromeric or telomeric location. In addition to the expected clustering of coding mutations in *SF3B1*, *TP53*, *NOTCH1* and *KLHL6*, occurring predominantly in IgHV^{unmut} patients, the remaining 108 regions included 21 clusters of non-coding mutations lying in active regulatory promoter or enhancer regions of genes expressed in CLL cells. The majority of these regions occurred in either the Ig loci (52%, 11/21) or within regulatory regions of known targets of SHM, including *BCL6*, *TCL1A*, *BTG2* and *BACH2*,^{53,54} and were more common in IgHV^{mut} patients (Figure 4). We were unable to find previously described mutations in the splice-site region of *NOTCH1*.¹⁸ This is likely due to their low incidence of ~2%.¹⁸

Third, we performed a further hotspot analysis to identify recurrently mutated regions and genes with fewer variants than are required to be classified as kataegis. This revealed *IKZF3* mutations in three IgHV^{unmut} patients and a further five with mutations in regulatory regions, only one of which was IgHV^{mut}. We also detected *SAMHD1* coding mutations in two IgHV^{unmut} cases and three mutations in active regulatory elements in two IgHV^{unmut} and one IgHV^{mut} case (Figures 4a and b and Supplementary Figures 2 and 3). Both *IKZF3* and *SAMHD1* have been identified as driver genes in CLL.^{16,17,44} Furthermore, we identified clusters of mutations within active enhancer and promoter regions of *ST6GAL1* in nine IgHV^{mut} patients and three IgHV^{unmut} patients. Overexpression of *ST6GAL1* has been linked to chemoresistance in leukaemia⁵⁵ and indeed two of the affected cases were confirmed chemorefractory with otherwise good-risk features. Mutations affecting the *PAX5* enhancer region have been recently described in CLL,^{18,56} and, indeed, in our cohort a single IgHV^{mut} patient, CLL351, harboured a mutation in this region. Additionally, we identified eight mutations within the boundaries of the *PAX5* gene, and which correlated with non-coding elements, in our cohort, comprising seven mutations across six IgHV^{unmut} patients and one mutation in one IgHV^{mut} patient. Six of these mutations were located in sites of transcription elongation, and the remaining two in promoter and enhancer regions (Supplementary Figure 4).

Finally, we focussed on the regulatory regions of genes with strong *a priori* relevance to CLL biology. This analysis was restricted to sites at active regulatory regions (Supplementary Methods) in genes expressed in CLL cells. Here, only instances that harboured mutations in at least two patients in a given region were counted. This analysis revealed a number of recurrently

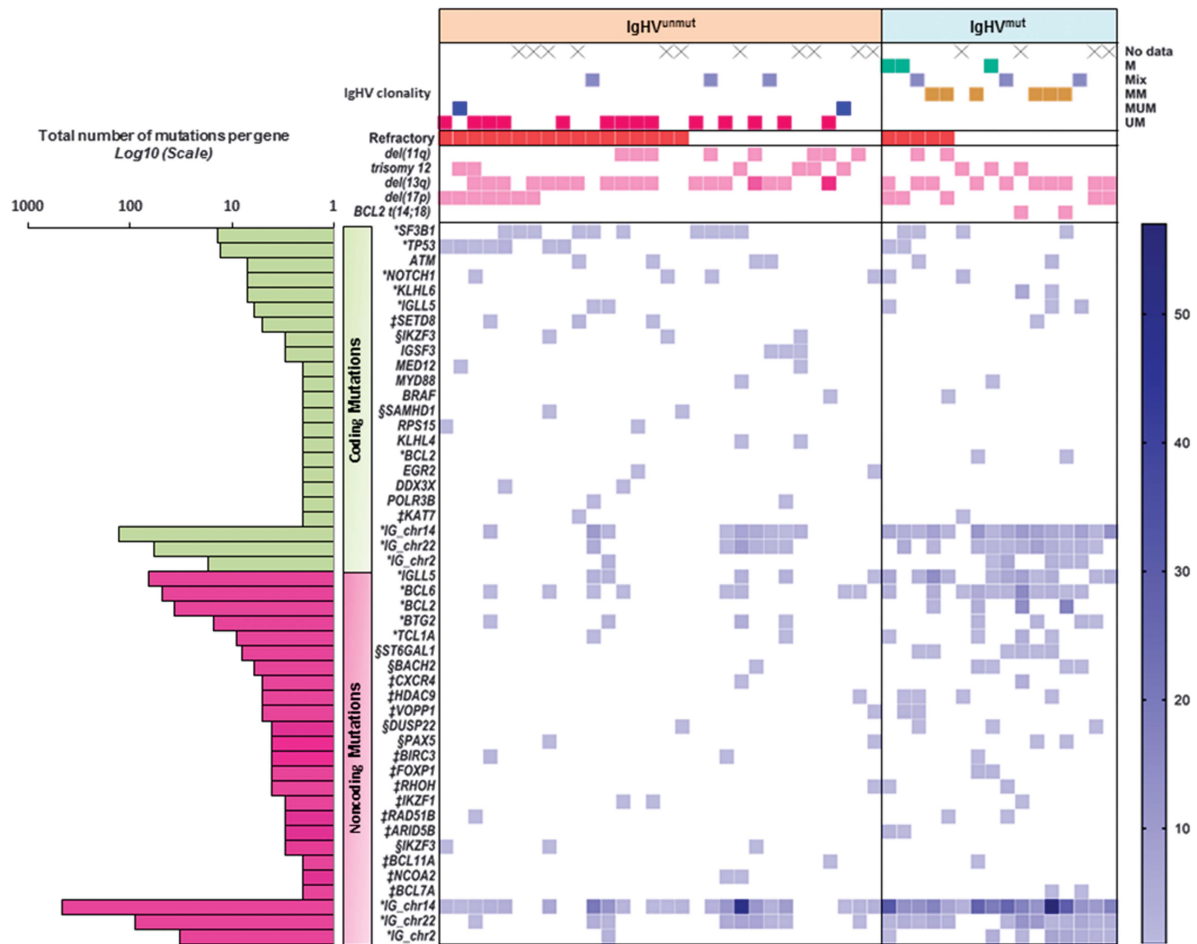


Figure 5. Overview of the mutational landscape in IgHV^{mut} and IgHV^{unmut} CLL. Top panel—Type and number of IgHV subclones present in each patient. Where several clones are present, IgHV status is determined by the identity of the dominant clone. Samples where only Sanger sequencing data were available are labelled as ‘not known’. Middle panels—Presence of copy number aberrations within the cohort. Lower panel—Incidence of both coding and non-coding mutations within the cohort. Colour spectrum (light to dark blue or light to dark pink) corresponds with mutational or CNA load per patient, respectively. *Genes containing kataeic mutations. †Genes with multiple mutations in regulatory regions and are involved in important B-cell pathways. ‡Genes with smaller mutational hotspots. Panel left: Number of mutations per gene across the entire cohort.

mutated active regulatory regions in genes involved in key pathways including B-cell development (*BCL6*, *IKZF1*, *PAX5*), nuclear factor-κB signalling (*TCL1A*, *BACH2*, *BIRC3*, *VOPPI*), NOTCH signalling (*HDAC9*) and DNA damage response (*BTG2*, *BCL2*) (Figure 5). With the exception of a subset of *BCL-2* promoter mutations that were linked to t(14;18) in two of three patients, paired RNA-seq data from the same patients did not reveal any differences in gene expression compared with patients without mutations in these regions (data not shown). As it can be difficult to uncouple treatment effect with biological effect, an association plot was constructed dividing data by chemoresistance and specifying previously treated patients (Supplementary Figures 5 and 6); however, no clustering was found within these groups.

Mutation signatures. Finally, we asked whether the difference in mutation distribution could arise as a consequence of the action of distinct mutagenic mechanisms. By using complex mathematical modelling, it has become possible to isolate a number of mutational patterns, or signatures, within the molecular landscape of cancer.^{29,30,42,57}

Although previously derived mutation signatures are extensive, they focus solely on exome data, and not whole genomes. Here, our aim was to compare the age, AID content and apolipoprotein B mRNA editing enzyme catalytic polypeptide (APOBEC) content

of our samples with the mutational signatures found in our complete data. Thus, for our initial analysis we derived novel mutation signatures. We used our WGS data to extract three distinct mutational signatures from our cohort. Tumour signature 1 (Tsig1) is dominated by C>T transitions in NpCpG and NpCpC contexts accounting for 56.8 and 5.5% of the signature, respectively (Figure 6a). Tumour signature 2 (Tsig2) is again defined primarily by C>T transitions in NpCpG trinucleotides; however, the occurrence of T>G transversions and T>C transitions at NpTpN sites differentiates it from Tsig1 (Figure 6a). Tsig3 is characterised by substitutions involving cytosine residues, with C>T, C>A and C>G variants at NpCpG trinucleotides accounting for 63% of the signature.

Previously, three mutational signatures were described in CLL,²⁹ attributed to the ageing process, and the ongoing presence of AID and APOBEC activity. To examine the relationship between these factors and the signatures in our data, we used a generalised linear model to correlate the proportion of each signature present in each sample with the levels of APOBEC and AID mutations, and the age of the patient (Figure 6b). We identified a strong positive correlation between Tsig1 and APOBEC mutations and a correlation between Tsig2 and the noncanonical AID signature.

We also examined our data for the presence of any of the 21 Alexandrov signatures, of which we identified 5 (1b, 5, 8, 9 and 16)

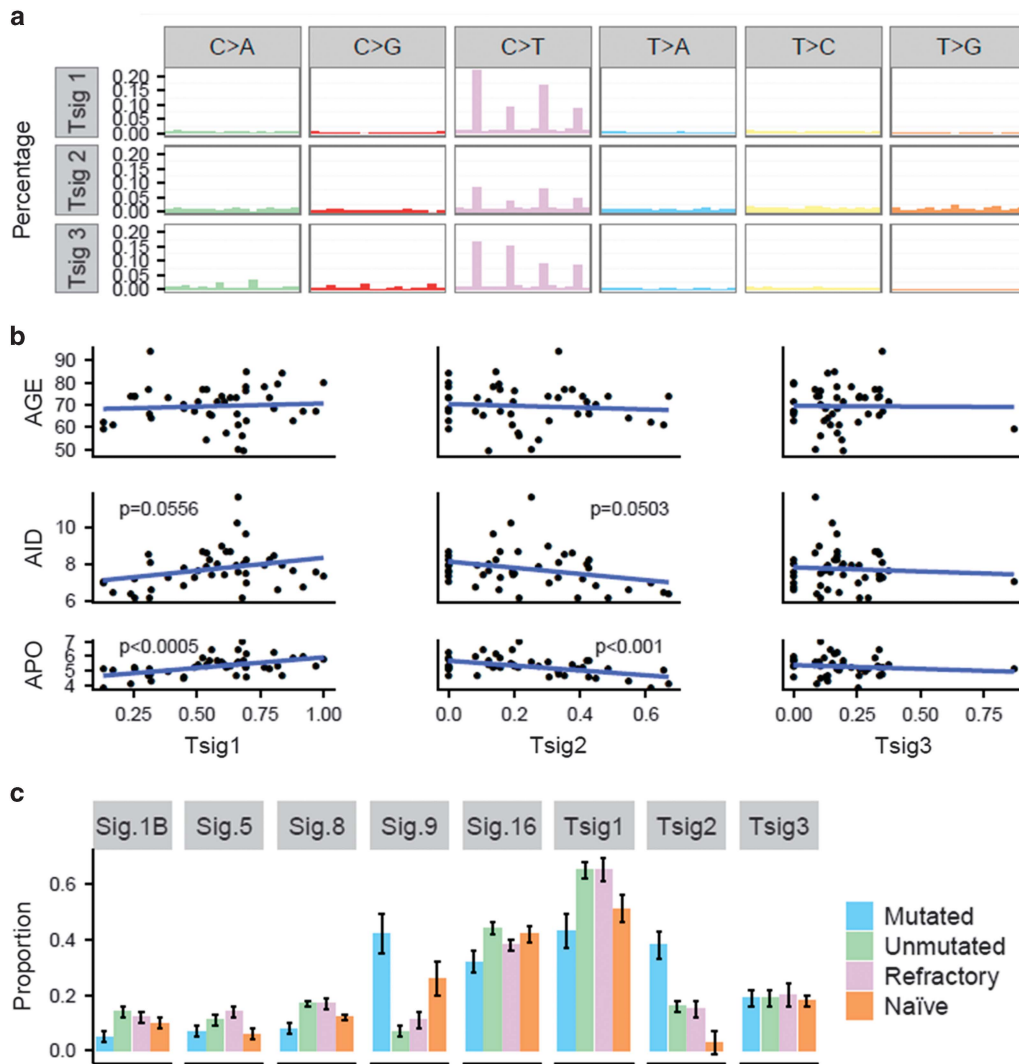


Figure 6. Mutation signature analysis. (a) Three mutation signatures identified across 46 patients using non-negative matrix factorisation (NMF). (b) Correlations between signatures identified in 46 patients and the corresponding age, or proportion of mutated canonical AID or APOBEC sites per subtracted somatic sample. Blue lines = regression lines, and *P*-values from the glm. (c) Proportions of mutation signatures from Alexandrov (2013), 29,43 where Sig.1B corresponds to Alexandrov Signature 1B, and so on, and signatures found across 46 patients.

(Figure 6c). Signature 1b is generally attributed to ageing, and showed a strong correlation with our Tsig1. However, in our cohort, neither signature 1b nor Tsig1 correlated with the age of the patient. Instead, we saw a significant increase in the proportion of Tsig1 in the refractory and IgHV^{unmut} patient groups. Owing to the overlap between these groups in our cohort, it was impossible to ascertain whether this correlation was independent. However, it strongly suggests that the underlying mechanism for the increase in Tsig1 in these patients might be exposure to previous chemotherapy and/or genomic instability. Tsig2-matched signature 9 is attributed to noncanonical AID activity and Ig hypermutation. As expected, both signature 9 and Tsig2 in our cohort are present at significantly higher levels in the IgHV-mutated cohort (Figure 6c). In summary, we were able to identify statistically significant differences in the proportion of mutation signatures between IgHV^{unmut} and IgHV^{mut} for Sig1b and Tsig1, Sig8, Sig9 and Tsig2, and Sig16.

DISCUSSION

Here we have used WGS to provide a comprehensive genome-wide description of the landscape of non-coding mutations of

both IgHV^{mut} and IgHV^{unmut} CLL. We reveal significant differences in the distribution of both somatic mutations and mutation signatures between these two subgroups. Previous WGS studies of CLL have focussed on good-risk treatment-naïve patient groups, such as those with monoclonal B-cell lymphocytosis or early stage CLL¹⁸ or IgHV^{mut} CLL with concurrent del(13q).⁵⁶ Here we have extended these published data sets and were able to compare it with the WGS data from poor-risk patients, many of whom were either IgHV^{unmut} and/or refractory to chemoimmunotherapy.

First, this genome-wide comparison of the mutation distribution between IgHV^{mut} and IgHV^{unmut} patients revealed a distinctive pattern for each subtype, with exonic CLL driver gene mutations being more common in IgHV^{unmut} patients, whereas mutations in regulatory elements of B-cell master regulators were more frequently observed in IgHV^{mut} patients. We developed and implemented a highly stringent filtering pipeline that excluded a large proportion of the genome, including repetitive, centromeric and telomeric domains to reduce the number of false-positive variants. Importantly, we only included mutations in DNase hypersensitivity sites or in regions of H3K4me3, H3K9ac, H3K4me1 or H3K27ac marks and complemented these with RNA-seq, and experimental CLL-specific data derived from

ChIP-seq and ATAC-seq (see Supplementary Methods). Annotations were assigned to the 'active non-coding element' classes of active promoter, strong enhancer or transcription transition sites from these primary CLL cells using chromHMM. This analysis revealed that at least 50% of somatically acquired mutation hotspots in regulatory regions of individual patients are located in genes found to also carry mutations in coding regions in CLL. In the case of non-coding mutations in *ATM*, these appeared to associate with altered RNA expression levels of these genes.

By performing a cohort-wide kataegis analysis, we were able to corroborate the findings of other groups with regard to the presence of mutations affecting the enhancer region of *PAX5* in IgHV^{mut} patients.^{18,56}

Transcription elongation (H3K36me3) and active promoter mutations were seen in *PAX5* in 6/27 (22%) of IgHV^{unmut} patients (Supplementary Figure 4). H3K36 trimethylation has been noted in yeast as a mechanism for the deacetylation of coding regions, thus stopping overactive transcription,⁵⁸ and there is some evidence to suggest that it might have a similar role in humans.⁵⁹ However, no effect on gene expression was found in our data (data not shown). We also found that 6 of 46 (13%) patients carried at least one mutation in the promoter region of *TCL1A* (Supplementary Figure 7). *TCL1A* is a direct activator of nuclear factor-κB. Translocations leading to *TCL1A* overexpression (t(14;14)(q11; q32)) by putting *TCL1A* expression under the control of the IgHV promoter have been described as rare events in lymphomas. Besides, the *TCL1A* promoter has previously been shown to display hypomethylation in CLL cells, providing an alternative mechanism for *TCL1A* upregulation in CLL.^{60,61} Moreover, microRNA dysregulation has also been proposed as a cause for *TCL1A* overexpression.⁶² In our series of patients, there was no difference in the *TCL1A* RNA expression in patients with or without mutations in the *TCL1A* promoter.

Importantly, we describe for the first time a number of somatically acquired genomic events that occurred predominantly or exclusively in patients in IgHV^{unmut} patients:

(1) We identified for the first time coding and non-coding mutations in *IKZF3* in almost 30% of IgHV^{unmut} patients (8 mutations in 8/27 patients), making *IKZF3* one of the most frequently mutated genes in high-risk CLL (Figure 4a). *IKZF3* is known to be overexpressed in CLL, and epigenetic modification of its promoter region has previously been described as one of the underlying mechanisms.⁶³ In the same study, overexpression or downregulation of *IKZF3* was shown to affect the expression of some Bcl-2 family members including *BCL-2*, thereby regulating apoptosis and cell survival. We can speculate that direct mutations in promoter and/or enhancer regions of *IKZF3* might represent either an alternative or complementary mechanism driving *IKZF3* deregulation in CLL. Further functional work will be required to understand their precise impact on CLL biology. In addition, mutations in the *IKZF3* paralogue *IKZF1* were found in active promoter regions in two IgHV^{unmut} patients (Supplementary Figure 8). Similar to *IKZF3*, *IKZF1* is a regulator of lymphocyte differentiation and has been linked to childhood B-cell precursor acute lymphoblastic leukaemia.⁶⁴

(2) Coding mutations in *SAMHD1* occurred in two IgHV^{unmut} patients, with three mutations in active regulatory regions in another three patients (Figure 4b). Somatic acquired germline mutations in the *SAMHD1* coding region have been shown to exist as founder events, regulating cell proliferation and survival, in relapsed and refractory CLL patients.^{17,44}

(3) *BIRC3* mutations in an active promoter or transcription elongation site occurred in 4/27 IgHV^{unmut} patients and one IgHV^{mut} patient (Figure 4c). *BIRC3* is a known cancer driver gene involved in nuclear factor-κB signalling. Exonic SNV mutations and deletions have been described previously and are associated with poor-risk disease.⁶⁵

(4) In all cases of regulatory mutations, further experimental analyses are required to fully link mutations to altered gene expression.

(5) Finally, we identify differences in the distribution of a number of mutation signatures, in particular the AID and aging signatures, pinpointing different pathogenic mechanisms of leukemogenesis. First, although the AID signature is more abundant in IgHV^{mut} CLL, it is also prevalent in IgHV^{unmut} CLL. These data are consistent with recent studies, which found that AID expression and full functional activity are intact in both IgHV^{mut} and IgHV^{unmut} CLL,³¹ and that canonical AID activity is an ongoing process in IgHV^{mut} patients.³² Conversely, IgHV^{unmut} and chemoimmunotherapy refractory CLL are dominated by the aging signature. This was independent of the age of the patient and implies that the increased incidence of driver mutations in this subgroup might be caused by repeated cell divisions, genomic instability and prior exposure to DNA-damaging agents rather than aberrant AID activity.

In conclusion, we provide evidence that in addition to recurrent mutations in the coding elements of the genome, non-coding mutations in known regulatory regions of critical B-cell transcription factors such as *PAX5* or *IKZF3* occur in significant subsets of CLL. On the basis of their mutation frequency in regulatory regions in several patients with IgHV^{unmut} CLL, we propose a number of genes including *IKZF3*, *BIRC3* and *SAMHD1* as warranting further functional investigation into the differences between IgHV^{mut} and IgHV^{unmut} CLL. Finally, we identify for the first time different dominant mutagenic mechanisms between these different types of CLL. The identification of the differences in the distribution of non-coding mutations between IgHV^{mut} and IgHV^{unmut} CLL is the first step towards an in-depth functional analysis. However, the fact that certain non-coding regions are recurrently targeted by mutations in a significant number of patients and that the majority of these occur in genes also targeted by mutations in the exome is in itself evidence for their functional relevance in CLL pathogenesis. Our data therefore supports the hypothesis that the biological and clinical differences observed between IgHV^{unmut} and IgHV^{mut} CLL are due, at least in part, to differences in the genomic footprint between these two subgroups and that regulatory mutations present a crucial avenue for further investigation.

CONFLICT OF INTEREST

JB and DB are employees of Illumina Inc., a public company that develops and markets systems for genetic analysis. The other authors declare no conflict of interest.

ACKNOWLEDGEMENTS

RA receives funding from the Saudi Arabian Government. This work was supported by the Oxford Partnership Comprehensive Biomedical Research Centre with funding from the Department of Health's National Institute for Health Research Biomedical Research Centres funding scheme. AS, JT and SJLK are supported also by the Health Innovation Challenge Fund (HICF-1009-026), a parallel funding partnership between the Wellcome Trust and the Department of Health. SJLK is also supported by the Wellcome Trust Core Award Grant (090532/Z/09/Z). The views expressed in this publication are those of the authors and not necessarily those of the Department of Health or the Wellcome Trust. EC and JIM-S are supported by the European Union's Seventh Framework Program through the Blueprint Consortium (grant agreement 282510) and by the Spanish Instituto de Salud Carlos III (grant ID PMP15/00007). JIM-S is also supported by Worldwide Cancer Research (grant number 16-1285). Additional annotation data were provided with permission from the ENCODE Consortium.

REFERENCES

- 1 Swerdlow SH, Campo E, Harris NL, Jaffe ES, Pileri SA, Stein H et al. *WHO Classification of Tumours of Haematopoietic and Lymphoid Tissues*, 4th edn. World Health Organization: Geneva, Switzerland, 2008.
- 2 Siegel R, Naishadham D, Jemal A. Cancer statistics, 2012. *CA Cancer J Clin* 2012; **62**: 10–29.

- 3 Döhner H, Stilgenbauer S, Benner A, Leupolt E, Kröber A, Bullinger L *et al*. Genetic aberrations and survival in chronic lymphocytic leukemia. *N Engl J Med* 2000; **343**: 1910–1916.
- 4 Seiler T, Döhner H, Stilgenbauer S. Risk stratification in chronic lymphocytic leukemia. *Semin Oncol* 2006; **33**: 186–194.
- 5 Puente XS, Pinyol M, Quesada V, Conde L, Ordóñez GR, Villamor N *et al*. Whole-genome sequencing identifies recurrent mutations in chronic lymphocytic leukaemia. *Nature* 2011; **475**: 101–105.
- 6 Schuh A, Becq J, Humphray S, Alexa A, Burns A, Clifford R *et al*. Monitoring chronic lymphocytic leukemia progression by whole genome sequencing reveals heterogeneous clonal evolution patterns. *Blood* 2012; **120**: 4191–4196.
- 7 Quesada V, Conde L, Villamor N, Ordóñez GR, Jares P, Bassaganyas L *et al*. Exome sequencing identifies recurrent mutations of the splicing factor SF3B1 gene in chronic lymphocytic leukemia. *Nat Genet* 2012; **44**: 47–52.
- 8 Zenz T, Vollmer D, Trbusek M, Smardova J, Benner A, Soussi T *et al*. TP53 mutation profile in chronic lymphocytic leukemia: evidence for a disease specific profile from a comprehensive analysis of 268 mutations. *Leukemia* 2010; **24**: 2072–2079.
- 9 Zenz T, Mohr J, Edelmann J, Sarno A, Hoth P, Heuberger M *et al*. Treatment resistance in chronic lymphocytic leukemia: the role of the p53 pathway. *Leuk Lymphoma* 2009; **50**: 510–513.
- 10 Zenz T, Kröber A, Scherer K, Häbe S, Bühler A, Benner A *et al*. Monoallelic TP53 inactivation is associated with poor prognosis in chronic lymphocytic leukemia: results from a detailed genetic characterization with long-term follow-up. *Blood* 2008; **112**: 3322–3329.
- 11 Rossi D, Brusca G, Spina V, Rasi S, Khiabani H, Messina M *et al*. Mutations of the SF3B1 splicing factor in chronic lymphocytic leukemia: association with progression and fludarabine-refractoriness. *Blood* 2011; **118**: 6904–6908.
- 12 Wang L, Lawrence MS, Wan Y, Stojanov P, Sougnez C, Stevenson K *et al*. SF3B1 and other novel cancer genes in chronic lymphocytic leukemia. *N Engl J Med* 2011; **365**: 2497–2506.
- 13 Rossi D, Rasi S, Fabbri G, Spina V, Fangazio M, Forconi F *et al*. Mutations of NOTCH1 are an independent predictor of survival in chronic lymphocytic leukemia. *Blood* 2011; **119**: 521–529.
- 14 Fabbri G, Rasi S, Rossi D, Trifonov V, Khiabani H, Ma J *et al*. Analysis of the chronic lymphocytic leukemia coding genome: role of NOTCH1 mutational activation. *J Exp Med* 2011; **208**: 1389–1401.
- 15 Rossi D, Rasi S, Spina V, Fangazio M, Monti S, Greco M *et al*. Different impact of NOTCH1 and SF3B1 mutations on the risk of chronic lymphocytic leukemia transformation to Richter syndrome. *Br J Haematol* 2012; **158**: 426–429.
- 16 Landau DA, Tausch E, Taylor-Weiner AN, Stewart C, Reiter JG, Bahlo J *et al*. Mutations driving CLL and their evolution in progression and relapse. *Nature* 2015; **526**: 525–530.
- 17 Clifford R, Louis T, Robbe P, Ackroyd S, Burns A, Timbs AT *et al*. SAMHD1 is mutated recurrently in chronic lymphocytic leukemia and is involved in response to DNA damage. *Blood* 2014; **123**: 1021–1031.
- 18 Puente XS, Beà S, Valdés-Mas R, Villamor N, Gutiérrez-Abril J, Martín-Subero JI *et al*. Non-coding recurrent mutations in chronic lymphocytic leukaemia. *Nature* 2015; **526**: 519–524.
- 19 Larrayoz M, Rose-Zerilli MJ, Kadalayil L, Parker H, Blakemore S, Forster J *et al*. Non-coding NOTCH1 mutations in chronic lymphocytic leukemia; their clinical impact in the UK CLL4 trial. *Leukemia* 2016; **31**: 510–514.
- 20 Hamblin TJ, Davis Z, Gardiner A, Oscier DG, Stevenson FK. Unmutated Ig V(H) genes are associated with a more aggressive form of chronic lymphocytic leukemia. *Blood* 1999; **94**: 1848–1854.
- 21 Tam CS, O'Brien S, Plunkett W, Wierda W, Ferrajoli A, Wang X *et al*. Long-term results of first salvage treatment in CLL patients treated initially with FCR (fludarabine, cyclophosphamide, rituximab). *Blood* 2014; **124**: 3059–3064.
- 22 Fischer K, Bahlo J, Fink AM, Goede V, Herling CD, Cramer P *et al*. Long-term remissions after FCR chemoimmunotherapy in previously untreated patients with CLL: updated results of the CLL8 trial. *Blood* 2016; **127**: 208–215.
- 23 Stamatopoulos B, Timbs A, Bruce D, Smith T, Clifford R, Robbe P *et al*. Targeted deep sequencing reveals clinically relevant subclonal IgHV rearrangements in chronic lymphocytic leukemia. *Leukemia* 2016; **31**: 837–845.
- 24 Rosenwald A, Alizadeh AA, Widhopf G, Simon R, Davis RE, Yu X *et al*. Relation of gene expression phenotype to immunoglobulin mutation genotype in B cell chronic lymphocytic leukemia. *J Exp Med* 2001; **194**: 1639–1647.
- 25 Klein U, Tu Y, Stolovitzky GA, Mattioli M, Cattoretto G, Husson H *et al*. Gene expression profiling of B cell chronic lymphocytic leukemia reveals a homogeneous phenotype related to memory B cells. *J Exp Med* 2001; **194**: 1625–1638.
- 26 Oakes CC, Seifert M, Assenov Y, Gu L, Przekopowicz M, Ruppert AS *et al*. DNA methylation dynamics during B cell maturation underlie a continuum of disease phenotypes in chronic lymphocytic leukemia. *Nat Genet* 2016; **48**: 253–264.
- 27 Stevenson FK, Krysov S, Davies AJ, Steele AJ, Packham G. B-cell receptor signaling in chronic lymphocytic leukemia. *Blood* 2011; **118**: 4313–4320.
- 28 Minden MD, Übelhart R, Schneider D, Wossning T, Bach MP, Buchner M *et al*. Chronic lymphocytic leukaemia is driven by antigen-independent cell-autonomous signalling. *Nature* 2012; **489**: 309–312.
- 29 Alexandrov LB, Nik-Zainal S, Wedge DC, Aparicio SAJR, Behjati S, Biankin AV *et al*. Signatures of mutational processes in human cancer. *Nature* 2013; **500**: 415–421.
- 30 Morganella S, Alexandrov LB, Glodzik D, Zou X, Davies H, Staaf J *et al*. The topography of mutational processes in breast cancer genomes. *Nat Commun* 2016; **7**: 11383.
- 31 Patten PEM, Chu CC, Albesiano E, Damle RN, Yan X-J, Kim D *et al*. IGHV-unmutated and IGHV-mutated chronic lymphocytic leukemia cells produce activation-induced deaminase protein with a full range of biologic functions. *Blood* 2012; **120**: 4802–4811.
- 32 Kasar S, Kim J, Impropio R, Tiao G, Polak P, Haradhvala N *et al*. Whole-genome sequencing reveals activation-induced cytidine deaminase signatures during indolent chronic lymphocytic leukaemia evolution. *Nat Commun* 2015; **6**: 8866.
- 33 ENCODE Project Consortium EP. The ENCODE (ENCyclopedia Of DNA Elements) Project. *Science* 2004; **306**: 636–640.
- 34 Hong EL, Sloan CA, Chan ET, Davidson JM, Malladi VS, Stratton JS *et al*. Principles of metadata organization at the ENCODE data coordination center. *Database* 2016; **2016**: baw001.
- 35 Thorsélius M, Kröber A, Murray F, Thunberg U, Tobin G, Bühler A *et al*. Strikingly homologous immunoglobulin gene rearrangements and poor outcome in VH3-21-using chronic lymphocytic leukemia patients independent of geographic origin and mutational status. *Blood* 2006; **107**: 2889–2894.
- 36 Raczy C, Petrovski R, Saunders CT, Chorny I, Kruglyak S, Margulies EH *et al*. Isaac: ultra-fast whole-genome secondary analysis on Illumina sequencing platforms. *Bioinformatics* 2013; **29**: 2041–2043.
- 37 Saunders CT, Wong WSW, Swamy S, Becq J, Murray LJ, Cheetham RK. Strelka: accurate somatic small-variant calling from sequenced tumor-normal sample pairs. *Bioinformatics* 2012; **28**: 1811–1817.
- 38 Ernst J, Kellis M. ChromHMM: automating chromatin-state discovery and characterization. *Nat Methods* 2012; **9**: 215–216.
- 39 Trapnell C, Pachter L, Salzberg SL. TopHat: discovering splice junctions with RNA-seq. *Bioinformatics* 2009; **25**: 1105–1111.
- 40 Rausch T, Zichner T, Schlattl A, Stütz AM, Benes V, Korbel JO. DELLY: structural variant discovery by integrated paired-end and split-read analysis. *Bioinformatics* 2012; **28**: i333–i339.
- 41 Lawrence MS, Stojanov P, Polak P, Kryukov GV, Cibulskis K, Sivachenko A *et al*. Mutational heterogeneity in cancer and the search for new cancer-associated genes. *Nature* 2013; **499**: 214–218.
- 42 Nik-Zainal S, Alexandrov LB, Wedge DC, Van Loo P, Greenman CD, Raine K *et al*. Mutational processes molding the genomes of 21 breast cancers. *Cell* 2012; **149**: 979–993.
- 43 Alexandrov LB, Nik-Zainal S, Wedge DC, Campbell PJ, Stratton MR. Deciphering signatures of mutational processes operative in human cancer. *Cell Rep* 2013; **3**: 246–259.
- 44 Landau DA, Carter SL, Stojanov P, McKenna A, Stevenson K, Lawrence MS *et al*. Evolution and impact of subclonal mutations in chronic lymphocytic leukemia. *Cell* 2013; **152**: 714–726.
- 45 Chapiro E, Leporrier N, Radford-Weiss I, Bastard C, Mossafa H, Leroux D *et al*. Gain of the short arm of chromosome 2 (2p) is a frequent recurring chromosome aberration in untreated chronic lymphocytic leukemia (CLL) at advanced stages. *Leuk Res* 2010; **34**: 63–68.
- 46 Forconi F, Rinaldi A, Kwee I, Sozzi E, Raspadori D, Rancoita PMV *et al*. Genome-wide DNA analysis identifies recurrent imbalances predicting outcome in chronic lymphocytic leukaemia with 17p deletion. *Br J Haematol* 2008; **143**: 532–536.
- 47 Brown JR, Hanna M, Tesar B, Werner L, Pochet N, Asara JM *et al*. Integrative genomic analysis implicates gain of PIK3CA at 3q26 and MYC at 8q24 in chronic lymphocytic leukemia. *Clin Cancer Res* 2012; **18**: 3791–3802.
- 48 Messina M, Del Giudice I, Khiabani H, Rossi D, Chiaretti S, Rasi S *et al*. Genetic lesions associated with chronic lymphocytic leukemia chemo-refractoriness. *Blood* 2014; **123**: 2378–2388.
- 49 Quesada V, Ramsay AJ, Rodríguez D, Puente XS, Campo E, López-Otin C. The genomic landscape of chronic lymphocytic leukemia: clinical implications. *BMC Med* 2013; **11**: 124.
- 50 Stankovic T, Weber P, Stewart G, Bedenham T, Murray J, Byrd PJ *et al*. Inactivation of ataxia telangiectasia mutated gene in B-cell chronic lymphocytic leukaemia. *Lancet (London, England)* 1999; **353**: 26–29.
- 51 Schaffner C, Stilgenbauer S, Rappold GA, Döhner H, Lichter P. Somatic ATM mutations indicate a pathogenic role of ATM in B-cell chronic lymphocytic leukemia. *Blood* 1999; **94**: 748–753.

- 52 Walker BA, Wardell CP, Murison A, Boyle EM, Begum DB, Dahir NM *et al*. APOBEC family mutational signatures are associated with poor prognosis translocations in multiple myeloma. *Nat Commun* 2015; **6**: 6997.
- 53 Khodabakhshi AH, Morin RD, Fejes AP, Mungall AJ, Mungall KL, Bolger-Munro M *et al*. Recurrent targets of aberrant somatic hypermutation in lymphoma. *Oncotarget* 2012; **3**: 1308–1319.
- 54 Pasqualucci L, Neumeister P, Goossens T, Nanjangud G, Chaganti RS, Küppers R *et al*. Hypermutation of multiple proto-oncogenes in B-cell diffuse large-cell lymphomas. *Nature* 2001; **412**: 341–346.
- 55 Ma H, Cheng L, Hao K, Li Y, Song X, Zhou H *et al*. Reversal effect of ST6GAL 1 on multidrug resistance in human leukemia by regulating the PI3K/Akt pathway and the expression of P-gp and MRP1. *PLoS One* 2014; **9**: e85113.
- 56 Rose-Zerilli MJ, Gibson J, Wang J, Tapper W, Davis Z, Parker H *et al*. Longitudinal copy number, whole exome and targeted deep sequencing of 'good risk' IGHV-mutated CLL patients with progressive disease. *Leukemia* 2016; **30**: 1301–1310.
- 57 Nik-Zainal S, Davies H, Staaf J, Ramakrishna M, Glodzik D, Zou X *et al*. Landscape of somatic mutations in 560 breast cancer whole-genome sequences. *Nature* 2016; **534**: 47–54.
- 58 Carrozza MJ, Li B, Florens L, Sukanuma T, Swanson SK, Lee KK *et al*. Histone H3 methylation by Set2 directs deacetylation of coding regions by Rpd3S to suppress spurious intragenic transcription. *Cell* 2005; **123**: 581–592.
- 59 Bartke T, Vermeulen M, Xhemalce B, Robson SC, Mann M, Kouzarides T. Nucleosome-interacting proteins regulated by DNA and histone methylation. *Cell* 2010; **143**: 470–484.
- 60 Garding A, Bhattacharya N, Haebe S, Müller F, Weichenhan D, Idler I *et al*. TCL1A and ATM are co-expressed in chronic lymphocytic leukemia cells without deletion of 11q. *Haematologica* 2013; **98**: 269–273.
- 61 Yuille MR, Condie A, Stone EM, Wilsher J, Bradshaw PS, Brooks L *et al*. TCL1 is activated by chromosomal rearrangement or by hypomethylation. *Genes Chromosomes Cancer* 2001; **30**: 336–341.
- 62 Pekarsky Y, Santanam U, Cimmino A, Palamarchuk A, Efanov A, Maximov V *et al*. Tc1 expression in chronic lymphocytic leukemia is regulated by miR-29 and miR-181. *Cancer Res* 2006; **66**: 11590–11593.
- 63 Billot K, Soeur J, Chereau F, Arrouss I, Merle-Beral H, Huang M-E *et al*. Dereglulation of Aiolos expression in chronic lymphocytic leukemia is associated with epigenetic modifications. *Blood* 2011; **117**: 1917–1927.
- 64 Boer JM, van der Veer A, Rizopoulos D, Fiocco M, Sonneveld E, de Groot-Kruseman HA *et al*. Prognostic value of rare IKZF1 deletion in childhood B-cell precursor acute lymphoblastic leukemia: an international collaborative study. *Leukemia* 2016; **30**: 32–38.
- 65 Rossi D, Fangazio M, Rasi S, Vaisitti T, Monti S, Cresta S *et al*. Disruption of BIRC3 associates with fludarabine chemorefractoriness in TP53 wild-type chronic lymphocytic leukemia. *Blood* 2012; **119**: 2854–2862.



This work is licensed under a Creative Commons Attribution-NonCommercial-NoDerivs 4.0 International License. The images or other third party material in this article are included in the article's Creative Commons license, unless indicated otherwise in the credit line; if the material is not included under the Creative Commons license, users will need to obtain permission from the license holder to reproduce the material. To view a copy of this license, visit <http://creativecommons.org/licenses/by-nc-nd/4.0/>

© The Author(s) 2018

Supplementary Information accompanies this paper on the Leukemia website (<http://www.nature.com/leu>)